Inorganic Chemistry

Article

pubs.acs.org/IC

Anion-Tunable Configuration Isomerism and Magnetic Coupling in a Tetranuclear Discrete, One-Dimensional (1D) Chiral Chain and 1D-Decker Copper(II) Complexes of a Carbohydrazine Derivative

Wei Huang,[†,‡] Yuchao Jin,[‡] Dayu Wu,*[,†,‡] and Genhua Wu[‡]

[†]Jiangsu Key Laboratory of Advanced Catalytic Materials and Technology, School of Petrochemical Engineering, Changzhou University, Changzhou, Jiangsu 213164, China

[‡]School of Chemistry & Chemical Engineering, Anqing Normal University, Anqing, Anhui 246011, China

Supporting Information

ABSTRACT: The reactions of ligand *N*′-[(pyridin-2-yl)methylene]-pyrazine-2-carbohydrazide (ppcd) with different copper salts (**1**, acetate; **2**, perchlorate; **3**, sulfate) in MeOH could afford one acetate-bridge tetranuclear discrete $[Cu_2(ppcd)(ac)_2(H_2O)(OH)]_2{\cdot}H_2O$ (**1**), one-dimensional (1D) chiral chain $[Cu(ppcd)]ClO_4$ (**2**), and a 1D-decker complex of a trinuclear copper(II) subunit, $Cu_3(ppcd)_2(H_2O)_4(SO_4)_2$ (**3**). Single-crystal X-ray analysis revealed that conformation isomerism of the ppcd ligand was associated with the configuration of −N−N− (trans or cis) and could induce the versatile coordination mode in the presence of different anions. The 1D chiral chain was interestingly obtained from the achiral rigid ligand in complex **2**. Magnetic studies indicated that the magnitude of the antiferromagnetic coupling can be tuned because of the configuration isomerism [compound **1** is practically diamagnetic at room temperature ($J \approx -1000$ cm^{-1}), with a strong antiferromagnetic one ($J = -255.4$ cm^{-1}) for **2** in the 1D uniform chain and an antiferromagnetic one ($J = -123.6$ cm^{-1}) for **3** within the trinuclear copper subunit].

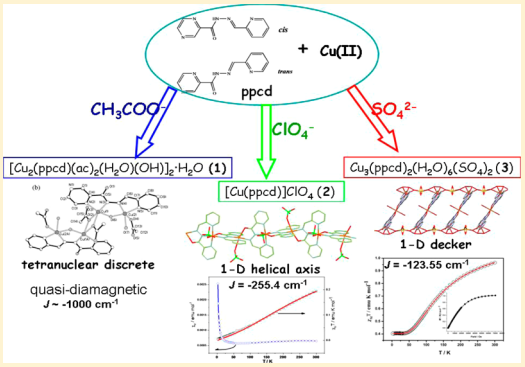

INTRODUCTION

During the past decades, the research of metal coordination architecture has been a dynamically thriving field and has attracted increasing interest because of the rich structure aesthetics and novel functionality.[1−3] There exist two major themes, namely, discrete molecular architecture and infinite coordination polymer, that have been well developed by virtue of the versatile coordination geometry of the metal ion in combination with different organic ligands.[4] The choice of synthetic organic ligands favoring a specific outcome of self-assembly is important with respect to the structures and properties of coordination architecture.[5] On the other hand, the production of a coordination compound is also affected by other factors, such as the solvent effect, pH, counteranion, etc.[6−8] Among them, some polymers coordinating with those containing nitrogen donors have been reported to have interesting properties, especially the triazole-, imidazole-, and benzimidazole-containing ligands.[9−12] Thompson's group did much work on the diazine-bridged ligands and reported that a variety of structure types could be observed on the basis of the free rotation of the copper coordination planes around the N−N single bond, which directly decides the magnitude of magnetic exchange via tuning of the overlap of the magnetic orbital.[5] However, the structure variation of coordination compounds arising from the configuration isomerism of the ligand skeleton would be helpful in understanding the relationship between the structure and functionality, but few examples are known.[13] Furthermore, magnetic coupling systems capable of utilizing the coexisting factors, such as anion and ligand isomerism, to synergistically influence the magnetic exchange are to be explored.

Representative in this work, different counterions with potential coordinative properties, such as barely or weakly coordinating perchlorate, sulfate, and bridging acetate, were selected to investigate the structure diversity of the carbohydrozone derivative and consequently explore the magnetic properties of different bridging modes between spin carriers. Meanwhile, the configuration tunability as well as the rich donor nature of the carbohydrazone ligand (Scheme 1) leads to a situation where different structural motifs occur through trans or cis configuration variation around the N−N bond by metal coordination of the terminal donor groups. This versatile ligand conformation can give rise to very different magnetic behaviors, dominated by an antiferromagnetic exchange in magnitude. Extension of the hydrazide framework to introduce the coordination pocket at both terminals leads to expansion of the coordination capacity of the ligand [e.g., *N*′-[(pyridin-2-yl)methylene]pyrazine-2-carbohydrazide (ppcd),

Received: June 3, 2013
Published: December 12, 2013

   dx.doi.org/10.1021/ic4014027 | *Inorg. Chem.* 2014, 53, 73−79

Scheme 1. Possible Conformation Isomers of the ppcd Ligand

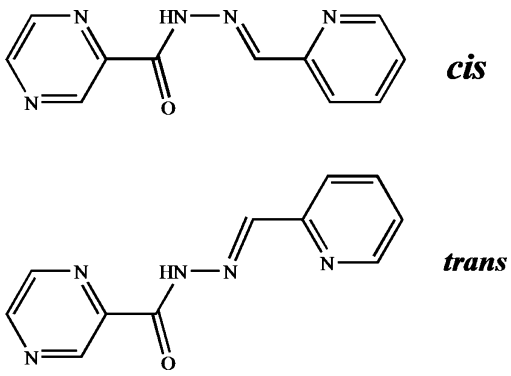

Scheme 1], the formation of anion-tunable structure diversity, and antiferromagnetic exchange with a diazine N_2 bridge.

Herein, we report the preparation, crystal structure, and magnetic properties of three compounds obtained from the reaction of copper(II) salt with ppcd in the presence of an auxiliary anion (ClO_4^-, **1**; CH_3COO^-, **2**; SO_4^{2-}, **3**). One tetranuclear discrete compound of formula $[Cu_2(ppcd)(ac)_2(H_2O)(OH)]_2 \cdot H_2O$ (**1**), one-dimensional (1D) compound $[Cu(ppcd)]ClO_4$ (**2**) with a chiral helical structure, and 1D-decker compound $Cu_3(ppcd)_2(H_2O)_6(SO_4)_2$ (**3**), respectively, were prepared by simply changing the anions. In addition, a cis-configuration ppcd ligand was observed for compound **1**; however, a trans-isomeric ppcd ligand was evidenced in compounds **2** and **3**, in which magnetic exchange in the different magnitudes was transmitted through a *cis*-N−N bridge ($J \approx -1000$ cm^{-1}) for **1** and a *trans*-N−N bridge ($J = -255.4$ and -123.6 cm^{-1}, respectively) for **2** and **3**.

EXPERIMENTAL DETAILS

Caution! *The perchlorate compound of metal ion is potentially explosive in organic solvents. Only a small amount of material should be prepared, and it should be treated with caution.*

Materials and Methods. The IR spectra were recorded (400−4000 cm^{-1} region) with a Nicolet Impact 410 FTIR spectrometer using KBr pellets. Elemental analysis of C, N, and H was performed with a Perkin-Elmer 240 analyzer. Magnetic susceptibility measurements of polycrystalline samples were measured over the temperature range 1.8−300 K with a Quantum Design MPMSXL7 SQUID magnetometer using an applied magnetic field of 2 kOe. Field dependences of magnetization were measured using a flux magnetometer in an applied field up to 70 kOe generated by a conventional pulsed technique. Data were corrected for the diamagnetic contribution calculated from Pascal's constants.

N′-[(Pyridin-2-yl)methylene]pyrazine-2-carbohydrazide (ppcd) was prepared according to the literature method.[14]

*$[Cu_2(ppcd)(ac)_2(H_2O)(OH)]_2 \cdot H_2O$ (**1**).* A methanolic solution (20 mL) containing ppcd (0.1 mmol, 0.0227 g) was slowly added to a methanolic solution (10 mL) containing $Cu(CH_3COO)_2 \cdot 6H_2O$ (0.2 mmol, 0.0600 g). After stirring at room temperature for 15 min, the resulting solution was filtered and allowed to stand undisturbed in air. Green block crystals were obtained by evaporating the concentrated solution at room temperature for several weeks. Yield: 36.7% (based on Cu). Anal. Calcd for $C_{15}H_{18}Cu_2N_5O_8$: H, 3.47; C, 34.42; N, 13.38. Found: H, 3.43; C, 34.49; N, 13.86.

*$[Cu(ppcd)]ClO_4$ (**2**).* Crystals were prepared by a layering method. A solution of ppcd (0.2 mmol) in CH_3OH (5 mL) was carefully layered upon a solution of $Cu(ClO_4)_2 \cdot 6H_2O$ (0.2 mmol) in H_2O (10 mL) in a sealed tube to allow slow diffusion in air at room temperature. After several days, green needle crystals of **2** suitable for X-ray analysis were adhered to the wall of the tube. Yield: 40.6% (based on Cu). Anal. Calcd for $C_{11}H_8ClCuN_5O_5$: C, 33.94; H, 2.07; N, 17.99. Found: C, 33.21; H, 2.21; N, 17.87.

*$Cu_3(ppcd)_2(H_2O)_6(SO_4)_2$ (**3**).* A solution of ppcd (0.2 mmol) in CH_3OH (5 mL) was layered on a solution of $Cu(SO_4)_2 \cdot 5H_2O$ (0.2 mmol) in H_2O (10 mL) in a sealed tube with very careful diffusion. After several days, green cubic crystals of **3** suitable for X-ray analysis were adhered to the wall of the tube. Anal. Calcd for $C_{22}H_{20}Cu_3N_{10}O_{16}S_2$: C, 28.25; H, 2.16; N, 14.98. Found: C, 28.34; H, 2.21; N, 15.21.

X-ray Crystallography. X-ray intensity data were measured at room temperature on a Bruker SMART APEX CCD-based diffractometer (Mo Kα radiation, $\lambda = 0.71073$ Å) using the *SMART* and *SAINT* programs. Raw data frame integration and Lp corrections were performed with *SAINT+*.[15] Final unit cell parameters were determined by least-squares refinement of strong reflections for the respective compounds **1**−**3**. The structures were solved by direct methods and refined on F^2 by a full-matrix least-squares method with *SHELXTL*, version 5.1.[16] All of the non-hydrogen atoms except the disordered solvent molecules were refined with anisotropic thermal displacement coefficients. Hydrogen atoms were located geometrically, whereas those of solvent molecules were found on Fourier difference maps, and all of the hydrogen atoms were refined in riding mode. Parameters for data collection and refinement of the compounds are summarized in Table 1.

Table 1. Crystallographic Data for Compounds 1−3

	1	2	3
formula	$C_{15}H_{18}Cu_2N_5O_8$	$C_{11}H_8ClCuN_5O_5$	$C_{11}H_{10}Cu_{1.50}N_5O_7S$
M_r	523.42	389.21	451.61
cryst syst	triclinic	tetragonal	triclinic
space group	$P\bar{1}$	$P4(1)$	$P\bar{1}$
a (Å)	9.1816(3)	8.3845(2)	7.3833(3)
b (Å)	10.7148(4)	8.3845(2)	8.5042(3)
c (Å)	11.2422(3)	19.2943(11)	12.6894(5)
α (deg)	62.331(3)	90	80.127(2)
β (deg)	85.798(3)	90	80.033(3)
γ (deg)	85.028(3)	90	79.988(2)
V (Å^3)	975.15(5)	1356.39(9)	764.53(5)
Z	1	4	1
D_{calcd} (g cm^{-3})	1.783	1.906	1.962
μ (mm^{-1})	2.236	1.843	2.292
R_{int}	0.0273	0.0979	0.0478
R1[a] [$I > 2\sigma(I)$]	0.0358	0.0865	0.0767
wR2[b] [$I > 2\sigma(I)$]	0.0960	0.2277	0.1855
S	1.064	1.072	1.234

[a] $R1 = \sum(|F_o| - |F_c|)/\sum|F_o|$. [b] $wR2 = \{\sum[w(F_o^2 - F_c^2)^2]/\sum[w(F_o^2)^2]\}^{1/2}$.

Structure Analysis. In order to obtain polynuclear or high-dimensional metal compounds, the carbohydrozone-containing ppcd ligand (Scheme 1) bearing N_2O tridentate coordination sites for chelating of the metal ions was prepared, which was easily deprotonated on the site of the imino group during metal coordination and was frequently treated as a mononegative charged ligand. The ease of availability of the ligand allowed us to systematically investigate the anion effects on the precise topography of the arrays.

*Compound **1**.* Compound **1** crystallizes in centric space group $P\bar{1}$, with the unsymmetric unit consisting of a copper dinuclear unit, as shown in Figure 1a, which is further connected via two 1,1-μ-bridged acetate groups to form a tetranuclear discrete copper with centrosymmetric structure (Figure 1b). Both copper(II) ions in **1** adopt a five-coordination environment with two nitrogen atoms from two bidentate ppcd ligands [N(4) and N(5)], one nonbridging acetate

dx.doi.org/10.1021/ic4014027 | Inorg. Chem. 2014, 53, 73−79

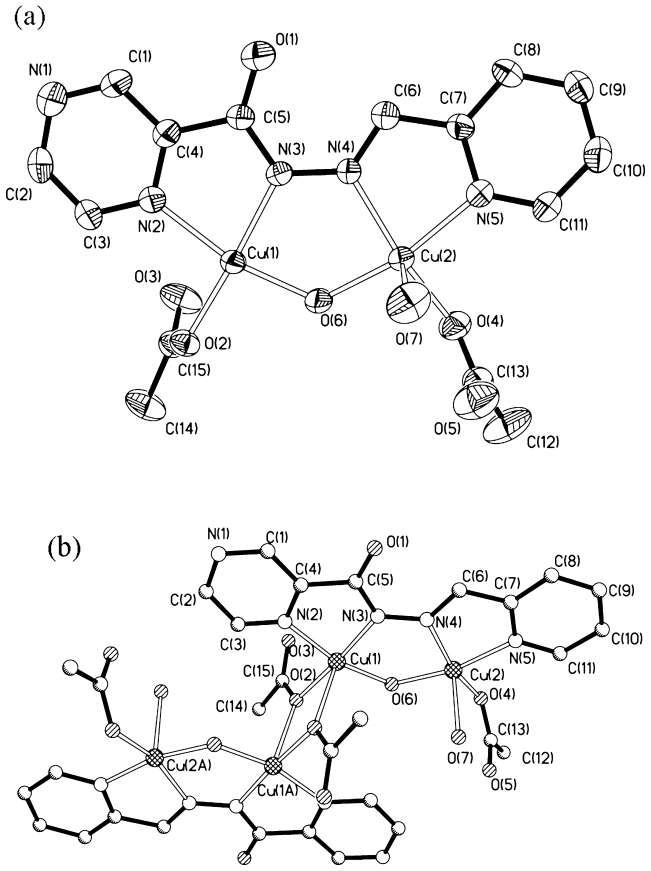

Figure 1. (a) Unsymmetric unit of compound **1**. (b) Crystal structure of the tetrameric compound **1** showing the atom numbering scheme. Ellipsoids are represented with 30% probability. The hydrogen atoms are omitted for clarity.

[O(4)], one water molecule [O(7)], and one bridging hydroxy [O(6)] for Cu(2); however, the coordination environment for Cu(1) shows little difference in that two bridging acetate oxygen atoms in addition to bidentate units [N(2) and N(3)] and one hydroxyl group [O(6)] fulfill the metal surroundings. Both copper centers could be described as a distorted square-pyramidal coordination configuration, which is indicated by values of the trigonality parameter $\tau = 0.17$ for Cu(1) and 0.08 for Cu(2) [$\tau = 1$ (trigonal bipyramid) and 0 (square pyramid), respectively, according to the definition by Addison et al.][17] In this sense, the topology of Cu(1) is slightly different from that of the Cu(2) center found in the parent compound **1**, where the five-coordination copper(II) environment of Cu(1) is much more distorted from the square pyramid. As shown in Figure 1a, an individual ppcd molecule acts as a chelating bis-bidentate ligand toward two copper(II) ions [with bite angles being 80.29(1) and 80.41(1)° for Cu(1) and Cu(2), respectively] together with one hydroxyl group at the equatorial position; consequently, the ligand skeleton adopts a *cis*-diazine configuration (Scheme 1). From the viewpoint of charge balance, the ppcd ligand loses one proton on the imine group and acts as an anionic ligand. The ligand (ppcd) as a whole is practically coplanar with a mean deviation from planarity of 0.001(2) Å. Two symmetry-related acetate groups (symmetry code: $1 - x, 1 - y, 1 - z$) bridge two dinuclear units at the Cu(1) position to constitute tetranuclear discrete chain with a Cu−O−Cu angle of ca. 103.89° (Figure 1b).

Compound **2.** Crystal structure X-ray analysis revealed that the asymmetric unit of **2** consists of a cationic $[Cu(ppcd)]^+$ along with a weakly coordinative perchlorate anion (Figure 2a). The coordination environment of the copper ion can be best described as a square pyramidal with trigonality parameter $\tau = 0.045$.[17] Each copper coordination sphere consists of three nitrogen donors from an individual ppcd ligand through one imino nitrogen, one pyridine nitrogen and one pyrazine nitrogen, and one imino nitrogen from another symmetry-related ligand with a comparable Cu−N bond (ca. 2.0 Å). The longer Cu−O contact is located at the apical position with a bond distance of 2.229 Å. The ClO_4^- anion can form a much longer Cu−O contact with a distance of 2.739 Å, that is weak coordination character. A view of the infinite helical chain structure of [Cu(ppcd)] (**2**) is shown in Figure 2b. Each ppcd ligand displays a bidentate/tridentate chelating mode to bridge the metal centers with the shortest intramolecular Cu···Cu separation of 4.878 Å. The NO bidentate unit of ppcd can chelate one copper ion with a O(1)−Cu(1)−N(4) angle of 75.75° in **2**. The strong chelation of ppcd in **2** enables the ligand to coordinate to two copper(II) ions to form an infinite chain structure around a 4_1 screw axis. The carbohydrozone groups bridge copper(II) into an infinite right-handed helical chain running along the *c* axis. The pitch length of the helical chain is 19.294(3) Å, which is identical with the *c*-axis length. The helix is generated around the crystallographic 4_1 screw axis (Figure 2b), which is consistent with compound **2** crystallizing in the $P4_1$ space group. Neighboring helical chains are parallel in the form of $\pi\cdots\pi$ stacking with a shortest atom···atom distance of 3.466 Å along the crystallographic *c* axis. From the viewpoint of the chirality source, it is interesting to observe that solid chirality can be achieved from the achiral ligand in compound **2**.

Compound **3.** The structure of complex **3** is built of a centrosymmetrical trinuclear $[Cu_3(ppcd)_2]$ cation (Figure 3a) and sulfate counteranions, which are weakly coordinated to terminal copper ions. The central copper(II) ion, which is located at a molecular inversion center, adopts an elongated octahedral environment, with two sets of NO bidentate groups consisting of two carbohydrozine oxygen atoms [O(1) and O(1A)] and two imine nitrogen atoms [N(4) and N(4A)] in equatorial positions [Cu(1)−O(1) = 1.975(3) Å and Cu(1)−N(4) = 1.975(4) Å] and two H_2O molecules [O(1W) and O(1WA)] occupying the axial positions [Cu−O(1) = 2.402(4) Å] (symmetry code A: $1 - x, -y, 1 - z$). Heavy disorder is observed for the sulfate anion. The sulfur atom S(1) [S(1A)] and one oxygen, O(14) [O(14A)], are distributed over two positions with equal site occupation factors (SOFs). Two oxygen atoms, including O(11) [O(11A) and O(11B)] and O(13) [O(13A) and O(13B)], are split into three parts, and they are refined with SOFs of 0.50, 0.25, and 0.25, respectively. The residual O(12) is located on the C_3 axis of the sulfate anion, and splitting is not observed. The terminal copper atom [Cu(2)] has, to our surprise, a rare disordered seven-coordination geometry with three nitrogen atoms [N(1), N(3), and N(5)] with Cu−N in the range 1.930(4)−2.036(4) Å, two disordered aqueous oxygen atoms [O(2W) and O(3W)] with Cu−O distances of 1.889(9) and 1.980(8) Å, respectively, and one oxygen atom, O(14), from sulfate forming a longer coordination sphere [Cu(2)−O(14) = 2.1547 Å]. A second, semicoordinated disordered sulfate oxygen atom [O(14A)] is situated at the remaining axial position [Cu(2)−O(14A) = 2.462(6) Å]. Two nearly planar ppcd ligands are located in the equatorial plane of the center copper Cu(1) and construct a trinuclear plane, with an atomic deviation from the mean plane being 0.0394 Å. As shown in Figure 3b, planes of neighboring trinuclear units are collected by disordered sulfate as bridging groups at the terminal copper ions such that trinuclear planes form a 1D-decker structure, with the interplanar distance being 6.36 Å. The Cu(1)···Cu(2) separation within the trinuclear unit across the *trans*-N−N− bridge is 4.713(2) Å, a value comparable to that observed in **2** because of similar bridging modes. The separation between two terminal copper ions is 9.426(3) Å.

Magnetic Analysis. The value of $\chi_M T$ at room temperature for **1** is only 0.034 cm^3 K mol^{-1} (Figure S1 in the Supporting Information, SI) [with χ_M being the magnetic susceptibility per two copper(II) ions], which is much reduced with respect to that expected for two magnetically isolated spin doublets [$\chi_M T = 2 \times 0.375$ cm^3 K mol^{-1} with $g = 2.0$] and corresponds practically to the situation of complete spin pairing caused by a very strong antiferromagnetic coupling between the copper(II) ions.

A careful investigation of the crystal structure revealed that two possible exchange pathways occur in **1**: (i) the combined diazine/

dx.doi.org/10.1021/ic4014027 | Inorg. Chem. 2014, 53, 73−79

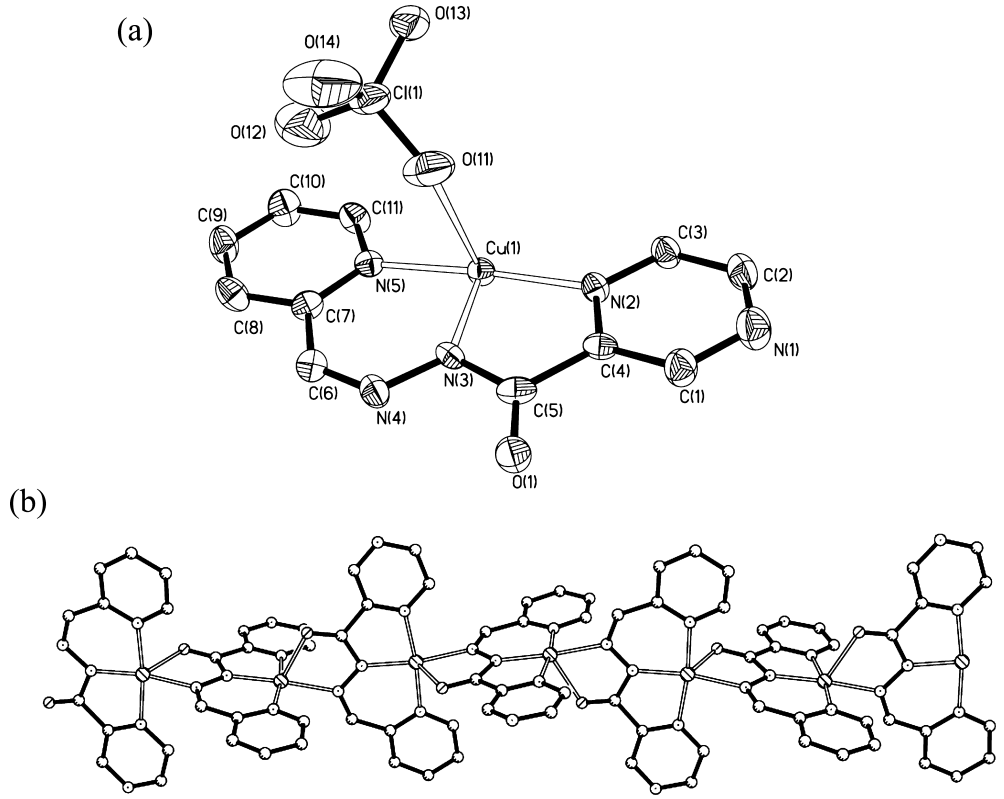

Figure 2. (a) Thermal ellipsoid plot of a copper(II) coordination environment. (b) Crystal structure of the 1D helical chain along the crystallographic *c* axis in complex **2** with a 4_1 screw axis with anions and the hydrogen atoms omitted for clarity. Ellipsoids are represented with 50% probability. The hydrogen atoms are omitted for clarity.

hydroxo bridge connecting both equatorial positions [Cu(1) and Cu(2)] and (ii) the double-oxygen bridges from the acetate group linking one equatorial position of Cu(1) and an axial position of another Cu(1A) from a neighboring symmetry-related dicopper(II) unit. The low efficiency of the longer axial Cu−O distance of 2.427 Å to mediate magnetic interactions between copper(II) ions, which had been demonstrated by previous magnetostructural studies,[18] allowed us to discard this exchange pathway and consider the first one as being responsible for the quasi-diamagnetic character of **1**. The exchange pathway between adjacent Cu(1) and Cu(2) ions involves double bridges by the combined diazine/hydroxo bridge at both equatorial positions in **1**, which can mediate the relatively large antiferromagnetic interactions in the reported copper(II) compound.[19−21] Because of the fact that the unpaired electron on Cu(1) and Cu(2) is localized in the equatorial plane, a good overlap between the magnetic orbitals ($x^2 - y^2$) of Cu(1) and Cu(2) in **1** is the origin of the strong antiferromagnetic coupling observed.[22−24] The structural parameters, including the values of Cu(1)···Cu(2) separation and the angle at the bridgehead hydroxo in **1** of 3.340(1) Å and 124.8(1)°, respectively, are reminiscent of those in a similar compound,[3,25] indicative of the comparable magnitude of the antiferromagnetic interaction between them. An orientative value of the magnetic coupling *J* in magnitude is estimated to be ca. −1000 cm^{-1} by the similar compounds $\{[Cu_2(dppn)(OH)(tcm)_2]\cdot tcm\}_n$ (J = −1180 cm^{-1})[3] and $[Cu_2(dppn)(OH)(ClO_4)_3(H_2O)_3]\cdot H_2O$ (J = ca. −1000 cm^{-1})[25] by Julve et al., having in common the combined N−N/hydroxo skeleton linking two copper(II) ions as in the case of compound **1**. The orbital complementary effects were pointed out to be responsible for these giant antiferromagnetic couplings between both bridges, a phenomenon that was studied for the first time by Nishida and Kida[26] and McKee et al.[27]

The magnetic properties of compound **2** in the form of both $\chi_M T$ and χ_M vs *T* plots [χ_M is the magnetic susceptibility for a copper(II) ion] are shown in Figure 4. $\chi_M T$ at 300 K is 0.19 cm^3 K mol^{-1}, a value that is more reduced than expected for one magnetically isolated spin doublet [$\chi_M T$ = 0.375 cm^3 K mol^{-1} with g = 2.00]. This value decreases very fast upon cooling, and it tends to vanish with decreasing temperature. These features are indicative of a strong antiferromagnetic interaction within a 1D copper chain.

The spin Hamiltonian for the chain of equally spaced copper(II) ions ($S = {}^1/_2$) to describe the isotropic interaction between nearest-neighboring ions is expressed in eq 1:

$$H = -J \sum_{i=1}^{n-1} [S_{A_i} \cdot S_{A_{i+1}}] \quad (1)$$

The analytical expression derived from the spin Hamilton mentioned above is as follows:[28]

$$\chi_M = \frac{Ng^2\beta^2}{kT} \frac{0.25 + 0.074975x + 0.075235x^2}{1 + 0.9931x + 0.172135x^2 + 0.757825x^3} \quad (2)$$

with $x = |J|/kT$.

The best-fit parameters for $\chi_M T$ versus *T* were g = 2.08(2) and J = −255.4 cm^{-1}, with the final agreement factor $R = 1.0 \times 10^{-5}$. The large negative *J* value confirms the presence of antiferromagnetic exchange coupling, which is transmitted by a single *trans*-N−N bridge.[13] It should be noted that the magnetic orbital is described as a $d_{x^2-y^2}$ type, and no spin density is residual on the d_{z^2} orbital. Therefore, the effective overlap of the magnetic orbitals ($d_{x^2-y^2}$ for copper(II) and p for N) leads to a strong magnetic interaction between the neighboring copper ions.

As shown in Figure 5, $\chi_M T$ for compound **3** at 300 K is 0.97 cm^3 K mol^{-1} [χ_M is the magnetic susceptibility per trinuclear copper(II) subunit], a value below what was expected for three noninteracting spin doublets ($3 \times 0.125 g^2 S(S+1)$ = 1.125 cm^3 mol^{-1} K with g = 2). Upon cooling, the value of $\chi_M T$ continuously decreases and reaches a plateau in the temperature range 2 K ≤ *T* ≤ 48 K with $\chi_M T$ = 0.40 cm^3 K mol^{-1} corresponding to an $S = {}^1/_2$ ground state (0.375 cm^3 K mol^{-1} for g = 2). This curve is typical of an intermediate intramolecular

dx.doi.org/10.1021/ic4014027 | Inorg. Chem. 2014, 53, 73−79

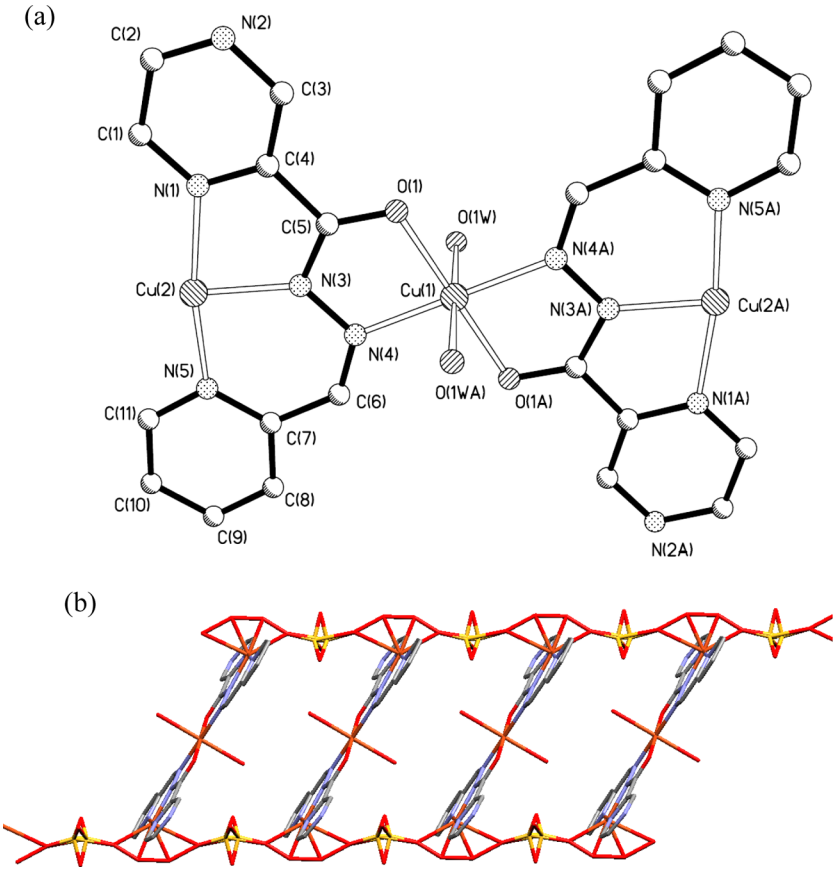

Figure 3. (a) View of the $[Cu_3(ppcd)_2(H_2O)_4]^{4+}$ trinuclear cationic fragment in **3** showing the selected atom numbering. Thermal ellipsoids are drawn at the 50% probability level. Symmetry code A: $1 - x, -y, 1 - z$. (b) Stick representation of the 1D-decker structure of the trinuclear unit in **3** connected by the disordered sulfate as the bridging groups at the terminal.

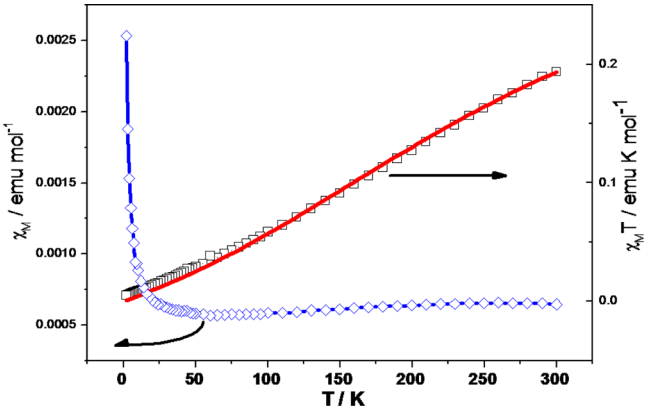

Figure 4. $\chi_M T$ and χ_M vs T plots for compound **2**. The solid line is the best-fit curve through eq 1 (see the text).

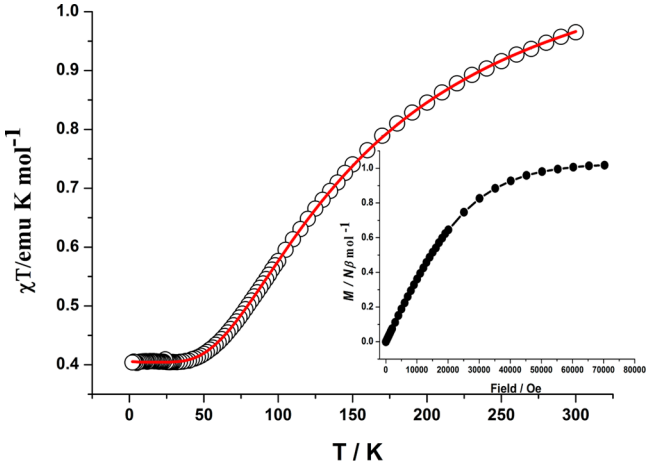

Figure 5. $\chi_M T$ vs T plot for complex **3**. The solid line is the best fit obtained with eq 4 (see the text). Inset: field dependence of magnetization measured at 2.0 K.

antiferromagnetic coupling in a copper(II) trimer and characteristic of the low-lying spin doublet (plateau of $\chi_M T$) being fully populated at $T \leq 48$ K. Indeed, the magnetization versus field data at 2.0 K (inset in Figure 5) tend to saturate at a value of 1.02 Nβ mol^{-1} that is expected for only an $S = {}^1/_2$ ground state ($M_{sat} = gS$). From the cystallographic observation that copper···copper separation by the disordered sulfate anions is as far as ca. 7.4 Å, which is ineffective in transmitting magnetic interactions, the magnetic data for **3** were consequently analyzed based on the following isotropic Hamiltonian for a copper(II) trimer:

$$H = -J_{12}S_1S_2 - J_{13}S_1S_3 \qquad (3)$$

The analytical expression that is derived from the spin Hamiltonian mentioned above is as follows:

$$\chi_M = \frac{N\beta^2}{4k(T-\theta)} \times \frac{[(4g_2 - g_1)/3]^2 + g_1^2 \exp(2x) + 10[(g_1 + 2g_2)/3]^2 \exp(3x)}{1 + \exp(2x) + 2\exp(3x)} \qquad (4)$$

dx.doi.org/10.1021/ic4014027 | Inorg. Chem. 2014, 53, 73−79

where $x = J/2kT$.

Considering the structural symmetry in compound **3**, $J = J_{12} = J_{13}$ is the exchange coupling parameter between adjacent copper(II) ions within the trimer, θ is the parameter accounting for the intermolecular interactions, and g_1 (central) and $g_2 = g_3$ (peripheral) are the local Landé factors. The magnetic coupling between the peripheral copper(II) ions (J_{23}), which are separated by 9.426(3) Å [Cu(2)···Cu(2A)], was not considered in the fitting expression. Best-fit parameters through eq 4 are $J = -123.6$ cm^{-1}, $g_1 \approx g_2 = 2.08$, $\theta = 0.00509$ K, and $R = 1.5 \times 10^{-6}$ [R is the agreement factor defined as $\sum[(\chi_M T_{obs} - \chi_M T_{calc})^2/\sum(\chi_M T_{obs})^2]^{1/2}$], which indicates that the calculated curve (solid red line in Figure 5) matches the magnetic data very well. The result is comparable to that of some diazine-bridged trinuclear copper compounds in the earlier study by Thompson et al.[5c] The principal feature responsible for the magnetic property of compound **3** is that the single N−N bond constitutes a direct linkage between adjacent copper(II) centers. Previous studies on dinuclear copper(II) complexes clearly indicated that the extent of exchange coupling through a N−N bond bridge is linearly dependent on the rotational angle of the copper magnetic planes relative to the single bond itself, which is a function of the relative orientation of the nitrogen p orbitals.[29] At large angles approaching a trans conformation, strong antiferromagnetic coupling is observed, while at low angles, the exchange becomes weaker with a changeover to ferromagnetic behavior at acute angles of around 80°. Compound **3** has a magnetic structural element with three copper centers connected by just N−N bonds. The magnetic plane of the central copper is defined by N(4), N(4A), O(1), and O(1A). The Cu−N−N−Cu torsional angle is 177.00°, which results in a full trans arrangement of the copper centers around the N−N bonds. The substantially large exchange parameter ($J = -123.6$ cm^{-1}) in this case is entirely consistent with this conformational feature, in addition to the presence of comparatively short overall Cu−N(O) bond lengths in the equatorial plane.

In conclusion, three new copper(II) compounds derived from the carbohydrazine ligand have been synthesized and structurally characterized. X-ray analyses revealed that the great versatility of this ligand upon coordination to a copper(II) metal ion and the coordination modes of copper(II) are influenced by the counteranions. The different coordinating abilities of anions likely contribute to structure variation. Compound **1** presents a center-symmetry anion-bridge tetranuclear unit consisting of binuclear molecules in which the ppcd ligand features *cis*-diazine bis-chelated carbohydrazine. For compound **2**, the ligand acts as a tridendate pocket and is adopted in the *trans*-diazine configuration. The neighboring copper centers are bridged by a *trans*-diazine group, which results in an unusual 1D chiral chain structure. However, in compound **3**, the planar trinuclear copper subunits are connected at the terminals through the disordered sulfate anion to construct a rare 1D-decker structure. Studies of the magnetic susceptibility revealed the quasi-diamagnetic character of **1**, which is associated with complete spin pairing through the combined diazine/hydroxo bridge because of very strong magnetic coupling between the copper(II) ions. Compound **2** can be treated as a 1D uniform magnetic chain with a strong coupling parameter ($J = -255.4$ cm^{-1}). Compound **3** is a trinuclear copper linear array, in which the copper ion is connected with a *trans*-N−N bridge ($J = -123.6$ cm^{-1}). To the best of our knowledge, very few examples of structure versatility induced by configuration isomerism along with the tuning of magnetic coupling were observed in the assembly process. Especially, the occurrence of **2** definitely confirms the possibility of building chiral coordination polymers from achiral tridendate carbohydrazine even with a less flexible coordinaton pocket. Further work on probing the chirality source of 1D polymeric metal compounds with the purpose of achieving a new chiral molecular magnet is underway.

■ ASSOCIATED CONTENT

Ⓢ Supporting Information

Crystallographic data (CIF files) for **1**−**3** and additional experimental data. This material is available free of charge via the Internet at http://pubs.acs.org.

■ AUTHOR INFORMATION

Corresponding Author

*E-mail: wudy@cczu.edu.cn.

Notes

The authors declare no competing financial interest.

■ ACKNOWLEDGMENTS

The authors are thankful for the anonymous reviewers' comments on the manuscript. This work was supported by Natural Science Foundation of China (Grants 21371010, 21001008, 21001007, and 21171008). D.W. also thanks Prof. J. Tao for kindly helping with SQUID measurements and State Key Laboratory of Physical Chemistry of Solid Surfaces, Xiamen University (Grant 201015), for support.

■ REFERENCES

(1) Xu, Z.; Thompson, L. K.; Matthews, C. J.; Miller, D. O.; Goeta, A. E.; Wilson, C.; Howard, J. A. K.; Ohba, M.; Okawa, H. *J. Chem. Soc., Dalton Trans.* **2000**, 69−77.

(2) (a) Sun, W.-W.; Cheng, A.-L.; Jia, Q.-X.; Gao, E.-Q. *Inorg. Chem.* **2007**, *46*, 5471−5473. (b) Yue, Y.-F.; Gao, E.-Q.; Bai, S.-Q.; He, Z.; Yan, C.-H. *CrystEngComm* **2004**, *6*, 549−555.

(3) Yuste, C.; Bentama, A.; Stiriba, S. E.; Armentano, D.; De Munno, G.; Lloret, F.; Julve, M. *Dalton Trans.* **2007**, 5190−5200.

(4) Thompson, L. K. *Coord. Chem. Rev.* **2002**, *233*−*234*, 193−206.

(5) (a) Xu, Z.; White, S.; Thompson, L. K.; Miller, D. O.; Ohba, M.; Okawa, H.; Wilson, C.; Howard, J. A. K. *J. Chem. Soc., Dalton Trans.* **2000**, 1751−1757. (b) Yonemura, M.; Okawa, H.; Ohba, M.; Fenton, D. E.; Thompson, L. K. *Chem. Commun.* **2000**, 817−818. (c) Zhao, L.; Thompson, L. K.; Xu, Z.; Miller, D. O.; Stirling, D. R. *J. Chem. Soc., Dalton Trans.* **2001**, 1706−1710. (d) Xu, Z.; Thompson, L. K.; Miller, D. O. *Chem. Commun.* **2001**, 1170−1171. (e) Xu, Z.; Thompson, L. K.; Miller, D. O. *J. Chem. Soc., Dalton Trans.* **2002**, 2462−2466. (f) Abedin, T. S. M.; Thompson, L. K.; Miller, D. O.; Krupicka, E. *Chem. Commu.* **2003**, 708−709. (g) Grove, H.; Kelly, T. L.; Thompson, L. K.; Zhao, L.; Xu, Z.; Abedin, T. S. M.; Miller, D. O.; Goeta, A. E.; Wilson, C.; Howard, J. A. K. *Inorg. Chem.* **2004**, *43*, 4278−4288.

(6) Li, J.-R.; Tao, Y.; Yu, Q.; Bu, X.-H. *Chem. Commun.* **2007**, 1527−1528.

(7) Pasán, J.; Sanchiz, J.; Lloret, F.; Julve, M.; Ruiz-Pérez, C. *CrystEngComm* **2007**, *9*, 478−487.

(8) Chen, C.-L.; Goforth, A. M.; Smith, M. D.; Su, C.-Y.; zur Loye, H.-C. *Inorg. Chem.* **2005**, *44*, 8762−8769.

(9) Hu, X.; Zeng, Y.-F.; Chen, Z.; Saňudo, E. C.; Liu, F.-C.; Ribas, J.; Bu, X.-H. *Cryst. Growth Des.* **2009**, *9*, 421−426.

(10) Stamatatos, T. C.; Dionyssopoulou, S.; Efthymiou, G.; Kyritsis, P.; Raptopoulou, C. P.; Terzis, A.; Vicente, R.; Escuer, A.; Perlepes, S. P. *Inorg. Chem.* **2005**, *44*, 3374−3376.

(11) Lan, Y.-Q.; Li, S.-L.; Fu, Y.-M.; Xu, Y.-H.; Li, L.; Su, Z.-M.; Fu, Q. *Dalton Trans.* **2008**, 6796−6807.

(12) Du, M.; Zhang, Z.-H.; Wang, X.-G.; Tang, L.-F.; Zhao, X.-J. *CrystEngComm* **2008**, *10*, 1855−1865.

(13) Bu, X.-H.; Liu, H.; Du, M.; Zhang, L.; Guo, Y.-M.; Shionoya, M.; Ribas, J. *Inorg. Chem.* **2002**, *41*, 1855−1861.

(14) Wu, D.; Zhang, X.; Huang, P.; Huang, W.; Ruan, M.; Ouyang, Z. W. *Inorg. Chem.* **2013**, *52*, 10976−10982.

(15) *SMART and SAINT, Area Detector Control and Integration Software*; Siemens Analytical X-ray Systems, Inc.: Madison, WI, 1996.

(16) Sheldrick, G. M. *SHELXTL VS.1, Software Reference Manual*; Bruker AXS, Inc.: Madison, WI, 1997.
(17) Addison, A. W.; Rao, T. N.; Reedijk, J.; van Rijn, J.; Verschoor, G. C. *J. Chem. Soc., Dalton Trans.* **1984**, 1349−1356.
(18) Ruiz, E.; Alemany, P.; Alvarez, S.; Cano, J. *J. Am. Chem. Soc.* **1997**, *119*, 1297−1303 and references cited therein.
(19) Inoue, M.; Kubo, M. *Coord. Chem. Rev.* **1976**, *21*, 1−27.
(20) Tandon, S. S.; Thompson, L. K.; Hynes, R. C. *Inorg. Chem.* **1992**, *31*, 2210−2214.
(21) Escuer, A.; Vicente, R.; Mernari, B.; El Gueddi, A.; Pierrot, M. *Inorg. Chem.* **1997**, *36*, 2511−2516.
(22) Ruiz, R.; Sanz, J.; Cervera, B.; Lloret, F.; Julve, M.; Bois, C.; Faus, J.; Muñoz, M. C. *J. Chem. Soc., Dalton Trans.* **1993**, 1623−1628.
(23) Ruiz, R.; Lloret, F.; Julve, M.; Muñoz, M. C.; Bois, C. *Inorg. Chim. Acta* **1994**, *219*, 179−186.
(24) Castro, I.; Faus, J.; Julve, M.; Lloret, M. F.; Verdaguer, M.; Kahn, O.; Jeannin, S.; Jeannin, Y.; Vaissermann, J. *J. Chem. Soc., Dalton Trans.* **1990**, 2207−2212.
(25) Mastropietro, T. F.; Marino, N.; Armentano, D.; De Munno, G.; Yuste, C.; Lloret, F.; Julve, M. *Cryst. Growth Des.* **2013**, *13*, 270−281.
(26) (a) Nishida, Y.; Kida, S. *J. Chem. Soc., Dalton Trans.* **1986**, 2633−2640. (b) Nishida, Y.; Takeuchi, M.; Takahashi, K.; Kida, S. *Chem. Lett.* **1985**, 631−634. (c) Nishida, Y.; Takeuchi, M.; Takahashi, K.; Kida, S. *Chem. Lett.* **1983**, 1815−1818.
(27) (a) McKee, V.; Zvagulis, M.; Reed, C. A. *Inorg. Chem.* **1985**, *24*, 2914−2919. (b) McKee, V.; Zvagulis, M.; Dagdigian, J. V.; Patch, M. G.; Reed, C. A. *J. Am. Chem. Soc.* **1975**, *97*, 4884−4899.
(28) Kahn, O. *Molecular Magnetism*; VCH: New York, 1993.
(29) Navarro, J. A. R.; Romero, M. A.; Salas, J. M.; Quirós, M.; Tiekink, E. R. T. *Inorg. Chem.* **1997**, *36*, 4988−4991.

dx.doi.org/10.1021/ic4014027 | *Inorg. Chem.* 2014, 53, 73−79